SUPPLEMENTARY FIGURE 1. **Co-expression of two independent RNAi constructs is more effective than either alone**. *A*, Average reduction in electropherogram A/G peak height ratios at 33 editing sites derived from head cDNA isolated from either transgene line alone or both transgenes driven by *elav*-Gal4 (n = 3 independent PCRs per site). Percentage reduction is relative to transgene(s)/+ controls. Although both dADAR RNAi constructs reduce levels of endogenous editing, combining both constructs elicits a significantly greater reduction in editing (value of % reduction is indicated in graph; ***: $p < 0.0005$, paired t-test). *Error bars*, S.E values. *B*, Example of synergistic effects on a high level editing site (site 6 of the Dα6 AChR mRNA). *C*, Graphical representation of percentage reduction in editing at 33 target adenosines following dADAR knock-down, plotted against initial level of editing in the transgenes/+ control background. Several adenosines edited at levels > 80% exhibit detectable levels of editing following dADAR knockdown, in contrast to adenosines edited at lower levels. However, highly edited adenosines may show distinct responses to dADAR knockdown. Two examples are circled in *C*, and representative examples of the corresponding electropherograms are shown in *D*. Editing at two adenosines in *Caα1D* and one in *shab* mRNA occur at similar levels (~ 100%). Following dADAR knock-down, editing at *Caα1D* sites 3 and 4 is abolished, yet editing at *shab* site 4 is only reduced to ~ 40%.

SUPPLEMENTARY FIGURE 2: **Near attainment of a full *dAdar* null phenocopy via simultaneous dADAR knockdown in neurons and muscle in a wild-type genetic background.** Graph shows number of beam breaks over 24 h in control and positive experimental genotypes. Values indicate magnitude relative to *dAdar* null flies (n = 10-11 vials per genotype). Flies heterozygous for both RNAi constructs do not significantly differ from w^{1118} controls, indicating a lack of transgene leak on locomotor activity. Locomotion is almost completely abolished following dADAR knockdown both neurons and muscle cells. *Error bars*, S.E values.

SUPPLEMENTARY FIGURE 3. **Effects of dADAR knockdown in cholinergic neurons on A-to-I editing in mRNAs encoding pre-synaptic release proteins.** *A*, Graph showing average editing levels in whole fly heads (n = 3-8 independent electropherograms) for 6 sites in 4 pan-neuronal transcripts. Pan-neuronal knockdown of dADAR abolishes editing at 5/6 sites and reduces *syt-1* site D by ~ 80%. Total head levels of editing in *syt-1* are not affected following dADAR knockdown in cholinergic neurons. In contrast, editing levels in *lap*, *dUnc-13* and *Stoned-B* (*Stn-B*) show clear reductions compared to transgenes/+ or driver/+ controls. *Error bars*, S.E values. **: $p < 0.005$; ***: $p < 0.0005$. *B*, Table showing % reductions in whole-head editing at all 6 sites following dADAR knockdown in cholinergic neurons. Significant reductions relative to both control backgrounds are shown in red. Values in black are either not significant or not reduced relative to both control backgrounds. *C-D*, Example electropherograms illustrating site-specific effects of dADAR knockdown in cholinergic neurons. Editing in *lap* is reduced by ~ 40% relative to transgenes/+ controls when both RNAi constructs are driven in cholinergic neurons, and abolished when driven pan-neuronally (*C*). In contrast, while editing at *syt-1* site D is dramatically reduced following pan-neuronal expression of both RNAi constructs, dADAR knockdown solely in cholinergic neurons has no significant effect on total head levels of editing (*D*).

SUPPLEMENTARY FIGURE 4: **A molecular reporter for cell-specific dADAR activity.** *A*, Strategy for construction of the reporter. Exon 9 of the *syt-1* mRNA contains four edited adenosines (sites A-D). The cis-acting sequences that direct editing of sites C and D have been defined, and are located in the downstream intron (E1 and E2). The genomic region encompassing exons 8-10 (with an HA-tag at the 3' terminal) was cloned into a pUAS vector, allowing spatial control of expression using the UAS-Gal4 system. We predicted that the

presence of E1 and E2 in the downstream intron should be sufficient to facilitate A-to-I editing at sites C and D in exon 9, as has previously been shown in vitro (11). Remarkably, when driven in the nervous system, not only was editing at both sites robustly detected, the pattern of editing at in the artificial construct (*syt-T*) was similar to that of the endogenous *syt-1* mRNA amplified from control head cDNA (w^{1118} males heterozygous for both *dAdar* RNAi constructs), albeit at a reduced level. When driven by *cha*-Gal4 (cholinergic neurons) or *elav*-Gal4 (pan-neuronal), site D exhibited higher levels of editing relative to site C (*B, C*). Editing in *syt-T* did not significantly differ when expressed solely in cholinergic neurons relative to all neurons (*C*). We tested the efficacy of *dAdar* knockdown in cholinergic neurons by co-expressing *syt-T* along with both *dAdar* RNAi constructs. Following such co-expression, editing at site C in *syt-T* was abolished, and editing at site D was also significantly reduced. The fact that pan-neuronal dADAR knockdown fails to abolish editing at site D in the endogenous *syt-1* mRNA (in contrast to most editing sites; Supp. Fig. 3) suggests that site D has a high affinity for dADAR, which may make complete knockdown of this site difficult. Nonetheless, this experiment directly demonstrates that dADAR knockdown is successfully occurring when driving *dAdar* RNAi constructs with the *cha*-Gal4 driver. *Error bars*, S.E values. ***: $p < 0.0005$.

SUPPLEMENTARY FIGURE 5: **Broad recapitulation of wild-type editing patterns via expression of 3/4 dADAR in a *dAdar* null background.** *A*, Levels of editing in the rescue genotype broadly correlate with wild-type editing levels. The degree of correlation is higher for mRNAs encoding voltage-gated ion channels (VGICs, *B*) relative to those encoding ligand-gated ion channels (LGICs, *C*).

SUPPLEMENTARY FIGURE 6: **Over-expression of 3/4 dADAR with *tubulin*-Gal4 in a *dAdar* null background does not further rescue editing levels.** *A*, expression of 3/4 dADAR is ~ 3-fold higher when driven with *tub*-Gal4 relative to *elav*-S (n = 2 independent western blots). *B*, Auto-editing levels in the 3/4 dADAR mRNA are similar at both levels of expression. *C*, For 36 editing sites tested, elevated expression of 3/4 dADAR does not further rescue editing to wild-type levels (n ≥ 3 independent PCRs for each site). *Error bars*, S.E.M values. *D*, Elevated expression of 3/4 dADAR does not shift the spectrum of Dα6 mRNAs towards higher levels of editing (number of cDNA clones sequenced: *5g1*; *elav*-S > 3/4 dADAR - 109; *5g1*; *tub*-Gal4 > 3/4 dADAR - 116).

SUPPLEMENTARY TABLE 1

Primer sequences used to amplify mRNA targets of dADAR.

GENE PRODUCT	PRIMER TYPE	SEQUENCE (5' – 3')
α2δ	Forward	CGTCCGGAATTCCACAATAC
	Reverse	CCTCCTTGCCAATCAGGTAG
	Sequencing	CGACGAGTCCGAAGGATATT
Caα1T	Forward	GTTGCTGCGAATCCTCAAAT
	Reverse	GTTGGTGGTCGAGGAGTCTG
	Sequencing	TGTGGCACTAATGACGTTCG
Caα1T	Forward	GCATCGATTCTATGGGCATT
	Reverse	CAGTGGACGTAGCACTCGAA
	Sequencing	TTGCCAACTGTATTGCCTTG
cpx	Forward	AGCTAAGCAGATGGTTGGAAA
	Reverse	TGCATGACACATTTTCCCTCT
	Sequencing	CCCCAAGAAGAGCCCAAT
Dα5	Forward	CACTGGGTGTTACCATCTTGC
	Reverse	CTACGAGACAATAATATGTGGTG
	Sequencing	ACTGGGTGTTACCATCTTGC
	Sequencing	CGTGCATCAAATCATCAACT
Dα6	Forward	AATCTGCGCTGGAATGAAAC
	Reverse	CAATGTGAAGCCCAGTAGGG
	Sequencing	TGGAATGAAACGGAATACGG
Dβ1	Forward	CAGTGCATCCGAAGATGAAG
	Reverse	GGCTGGCAGGTAAAATACCA
	Sequencing	AAGATGAAGAGCGCTTGGTG
Dβ2	Forward	GACCTACAATGGTGCCCAAG
	Reverse	CACATCGATCTCGTTGGTGT
	Sequencing	CCCAAGTGGATCTGAAGCAT
DSC1	Forward	GCAAGGAATGCGGATTGTAG
	Reverse	GCGTTGCTCACTTCCAGAAT
	Sequencing	CGGATCGTTCTTCACACTGA
DopEcR	Forward	GGTGCCCTTCTCCGTGTAT
	Reverse	TTGAGGAGAATGAAAATCTAAATCTAA
	Sequencing	GACCGGAGAATGGATGTACG
eag	Forward	CAATACAGCTGGCTGTGGAA
	Reverse	TCACCCTTCTCGACATCACTT
	Sequencing	GACGGCCCTATATTTCACCA
	Sequencing	GCGACGAAATTTGGAGAAGA
DmGluCl	Forward	GGCAGCGGACACTATTTCTG
	Reverse	GCATCTAAACTGGCCTGCTC

	Sequencing	CTGACTATGGCGGGACCA
	Sequencing	CCTACCTCGCTTCACACTGG
lap	Forward	CGATGCGTTGGATCTTTACA
	Reverse	GGACAGCCAAGTATGATGGG
	Sequencing	TTGTTAGATGCCTTGGAGCA
para	Forward	CATTGGTGCAAATCGAACAA
	Forward	CGACCATTCAAGGACGAGAG
	Reverse	GCTCCGAATGGACATCTTCT
	Reverse	GTAACGATCGAGGGTCATGG
	Sequencing	CGCTGAACATGAAAAGCAGA
	Sequencing	CATTATTCATGCACACGACGA
	Sequencing	GATCGAGGGTCATGGTGAAC
rdl	Forward	CATGCTGGGTGACGTAAACA
	Reverse	CATACCGACGCCCACATT
	Sequencing	CGGAGTCACCATGTATGTGC
	Sequencing	TGCCCCAATTTAAGGTCTTG
shab	Forward	GAAGGTAAATGCGCCGAGTA
	Reverse	GTCCGTTTGCGAGAGATTGT
	Sequencing	GGAAACGAATAAGAATGCAACG
shaker	Forward	CTGGTCATGGCTTTGGTGGCGGACC
	Reverse	CCGTGTGATCAGTCAGACCTGGCG
	Sequencing	GGATCTGTGATGTCAGGCACCTCG
	Sequencing	CGAGGTGCCTGACATCACAGATCC
stoned-B	Forward	TCAAGGGTATCGAGCGAATC
	Reverse	GGCCAAGATGCCTTTGATAA
	Sequencing	TGCATACACCACACATCAGC
syt-1	Forward	GCTGCGCTACGTGCCGACCGCCGG
	Reverse	GTAGTCCACGACGGTCACAACGAG
	Sequencing	GCTGCGCTACGTGCCGACCGCCGG
dUnc-13	Forward	TGGACAGTTATCAGCATCTTCAA
	Reverse	ATTCGTGGCTCCAAACTGAT
	Sequencing	GCTGTGGACATGAAGTACGC

SUPPLEMENTARY TABLE 2

Editing levels in wild-type (Canton-S) males and *dAdar* null males expressing 3/4 dADAR driven by *elav*-S or *tub*-Gal4. Values represent mean ± S.E. n = 3-12 independent PCRs from at least n = 3 independent RT reactions.

Editing site	Canton-S	*5g1*; *elav*-S > 3/4 dADAR	*5g1*; *tub*-Gal4 > 3/4 dADAR
α2δ site 1	85.2 ± 0.7	62.9 ± 2	25.4 ± 1.2
α2δ site 2	30.4 ± 0.3	5.8 ± 0.3	1.5 ± 0.2
α2δ site 3	37.3 ± 0.9	10.9 ± 0.5	4.6 ± 0.9
Caα1D site 1	34.4 ± 1.2	29.7 ± 0.8	
Caα1D site 2	86.7 ± 1	76 ± 1.6	
Caα1D site 3	93 ± 0.7	66.6 ± 1.1	
Caα1D site 4	94.2 ± 0.8	66.1 ± 1	
Caα1D site 5	98.9 ± 1.1	76.3 ± 0.4	
Caα1T site 1	87 ± 2.2	41.4 ± 2	
cpx site 1	59 ± 0.4	24.4 ± 0.3	
cpx site 2	19.5 ± 4.6	6.3 ± 2.2	
cpx site 3	39.3 ± 1.8	13.7 ± 1.5	
Dα5 site 1	90.7 ± 0.2	32.3 ± 1	
Dα5 site 2	90 ± 0.1	30 ± 0.5	
Dα5 site 3	99.3 ± 0.5	41.4 ± 0.5	52.9 ± 2.4
Dα5 site 4	41.9 ± 1	4 ± 0.5	5.1 ± 0.8
Dα5 site 5	41.6 ± 0.9	5.9 ± 0.5	4.7 ± 0.8
Dα5 site 6	74.1 ± 0.3	18 ± 0.7	13.9 ± 0.7
Dα5 site 7	19.3 ± 0.4	5.2 ± 0.5	4.8 ± 0.6
Dα5 site 8	79.9 ± 0.7	22.6 ± 0.9	20.7 ± 1
Dα6 site 1	5.7 ± 0.4	2.1 ± 0.3	0
Dα6 site 2	16 ± 0.6	7.1 ± 0.5	9.8 ± 1.6
Dα6 site 3	0	0	
Dα6 site 4	74.8 ± 1.3	51.6 ± 3.8	42.6 ± 2
Dα6 site 5	78.2 ± 0.8	56.6 ± 5.8	46.9 ± 1.7
Dα6 site 6	79.2 ± 1	76.5 ± 1.6	72.3 ± 1
Dα6 site 7	51.1 ± 1.1	27.2 ± 0.6	15.4 ± 0.5
Dβ1 site 1	76.2 ± 0.9	35.3 ± 1.7	
Dβ1 site 2	86.8 ± 1.3	20.9± 1.6	
Dβ1 site 3	30.8 ± 1.2	0.6 ± 0.6	
Dβ1 site 4	99.2 ± 0.4	37 ± 1	

Dβ2 site 1	30.2 ± 0.3	23.9 ± 1.7	
Dβ2 site 2	30.3 ± 0.8	19.2 ± 4.2	
dsc1 site 1	64.6 ± 0.9	20.1 ± 2.2	14.9 ± 0.9
DopEcR site 1	5 ± 0.5	1.8 ± 0.05	0.9 ± 0.6
DopEcR site 2	5 ± 0.6	0	0.8 ± 0.8
DopEcR site 3	13.4 ± 0.2	9.7 ± 0.3	6.1 ± 1.6
DopEcR site 4	32.5 ± 0.3	23.3 ± 0.8	22.1 ± 3.9
DopEcR site 6	4.3 ± 0.6	2.4 ± 0.5	3.5 ± 1.7
DopEcR site 7	4.8 ± 0.6	1.7 ± 0.8	1.3 ± 1.3
DopEcR site 8	50.7 ± 0.6	22 ± 0.5	16.2 ± 3.5
DopEcR site 9	78.7 ± 1	46.7 ± 0.3	29.4 ± 4.4
DopEcR site 10	84.2 ± 0.3	61.9 ± 0.3	44.9 ± 4.4
eag site 1	65.9 ± 3.8	55.3 ± 2.4	
eag site 2	86.9 ± 0.2	70.3 ± 0.3	
eag site 3	15.6 ± 0.4	16.2 ± 0.3	
eag site 4	80.8 ± 0.7	71.9 ± 0.6	
eag site 5	9.1 ± 0.4	5.4 ± 0.6	
eag site 6	69.4 ± 0.4	47.8 ± 0.8	
DmGluCl site 1	70.2 ± 1.1	33.3 ± 0.6	
DmGluCl site 2	97.7 ± 0.8	54.2 ± 0.8	
DmGluCl site 3	65.4 ± 0.2	22.2 ± 0.7	
lap site 1	92.2 ± 2.5	27.1 ± 1	14.2 ± 0.5
para site 1	72.7 ± 5	30.1 ± 2.4	
para site 8	51.5 ± 1.5	18.7 ± 1.3	
para site 9	6.1 ± 0.5	1.8 ± 1.8	
para site 10	31.6 ± 0.5	6.9 ± 0.6	
para site 11	47.8 ± 3.3	18.5 ± 0.7	
para site 12	9.7 ± 0.4	0.5 ± 0.4	
para site 13	6.4 ± 0.9	1.3 ± 0.6	
para site 14	47.3 ± 1.4	16.6 ± 0.9	
para site 15	5.3 ± 0.9	0	
para site 16	1.8 ± 1	0	
rdl site 1	13.5 ± 1	1 ± 0.8	3.7 ± 0.5
rdl site 2	60.2 ± 0.5	23.5 ± 1.3	25 ± 2.9
rdl site 3	94.2 ± 3.5	73.1 ± 2.5	65.2 ± 0.7
rdl site 4	16.4 ± 3.5	1.3 ± 1	0.4 ± 0.4
rdl site 5	1.4 ± 0.01	0	
rdl site 6	10.3 ± 0.4	1.8 ± 1.1	

shab site 1	74.2 ± 1.5	51.2 ± 3	
shab site 2	89.2 ± 0.6	67.8 ± 3.1	
shab site 3	88.4 ± 1.6	68 ± 1.3	
shab site 4	95.4 ± 0.8	84.3 ± 0.5	
shab site 5	78.2 ± 0.6	61.8 ± 0.4	
shab site 6	72.7 ± 1.9	56 ± 1.8	
shab site 7	94.5 ± 1.5	75.2 ± 1.6	
shaker site 1	4.5 ± 0.6	0	2.6 ± 0.1
shaker site 2	3.8 ± 0..9	0	2 ± 0.2
shaker site 3	48.8 ± 1.7	47.1 ± 0.9	46 ± 1.7
shaker site 4	33.3 ± 1.6	26.9 ± 2	18.2 ± 2
shaker site 5	84.3 ± 2.6	46.1 ± 3	43.7 ± 0.6
shaker site 6	70.1 ± 0.9	33.2 ± 1.7	23.8 ± 0.9
stoned-B site 1	78.4 ± 1.9	49.9 ± 2.1	
syt site 2	38.3 ± 1.1	13.5 ± 1.8	
syt site 3	48.4 ± 6.1	20.6 ± 2.1	
syt site 4	85.5 ± 1.4	61.7 ± 1.9	
dUnc-13 site 1	64.6 ± 0.5	32.7 ± 1.9	

SUPPLEMENTARY TABLE 3

Sites edited by 3/4 dADAR to > 75% of wild-type		Sites edited by 3/4 dADAR to < 25% of wild-type	
Caα1D site 1	VGIC	Dα5 site 4	LGIC
Caα1D site 2	VGIC	Dα5 site 5	LGIC
Caα1D site 5	VGIC	Dα5 site 6	LGIC
eag site 1	VGIC	Dβ1 site 2	LGIC
eag site 2	VGIC	Dβ1 site 3	LGIC
eag site 4	VGIC	*rdl* site 1	LGIC
shab site 2	VGIC	*rdl* site 4	LGIC
shab site 3	VGIC	*rdl* site 6	LGIC
shab site 4	VGIC	α2δ site 2	VGIC
shab site 5	VGIC		
shab site 6	VGIC		
shab site 7	VGIC		
shaker site 3	VGIC		
shaker site 4	VGIC		
Dα6 site 6	LGIC		
Dβ2 site 1	LGIC		
rdl site 3	LGIC		

SUPPLEMENTARY FIGURE 1

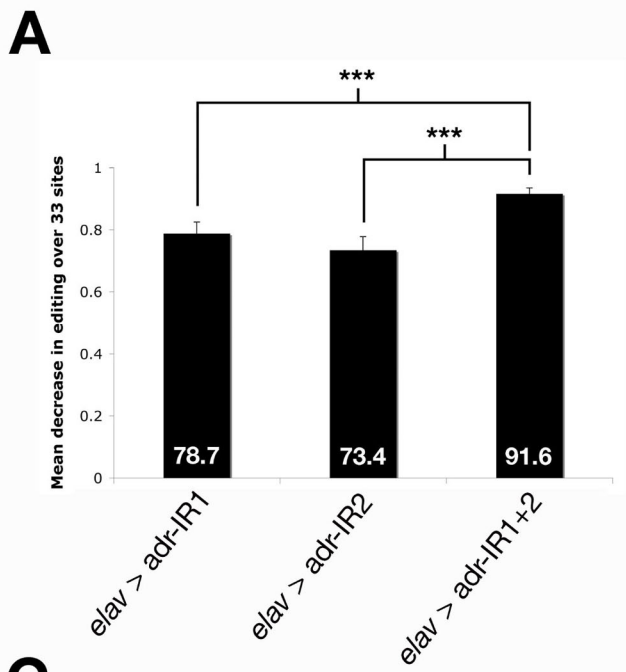

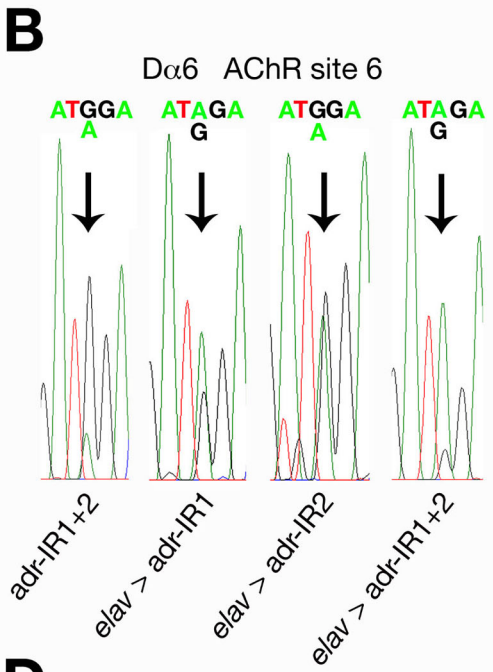

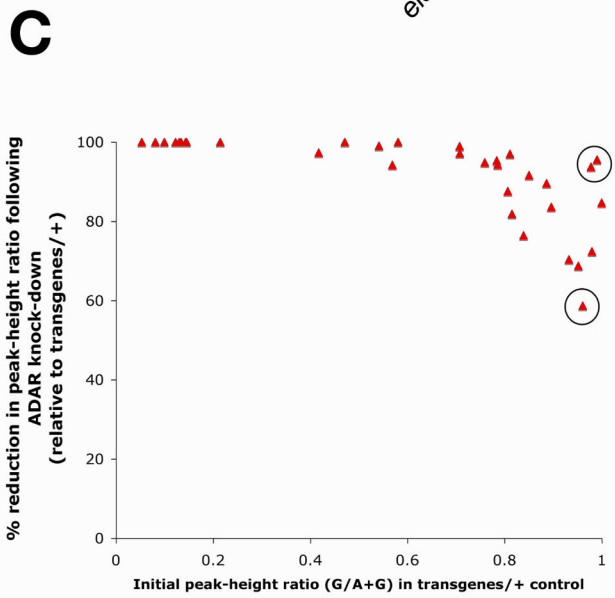

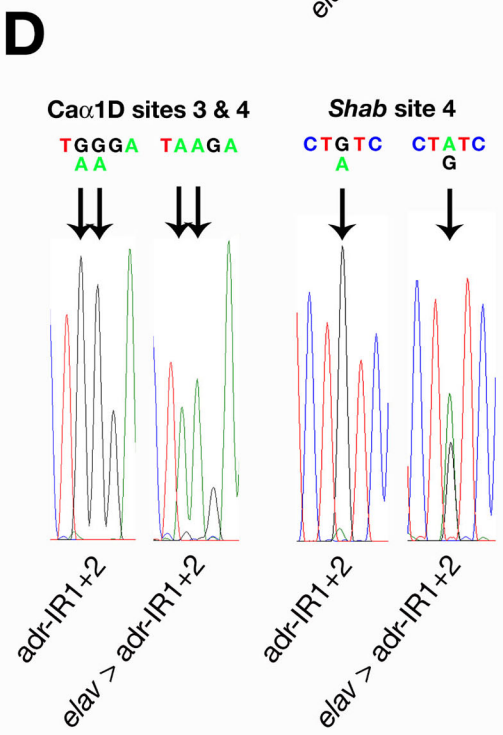

SUPPLEMENTARY FIGURE 2

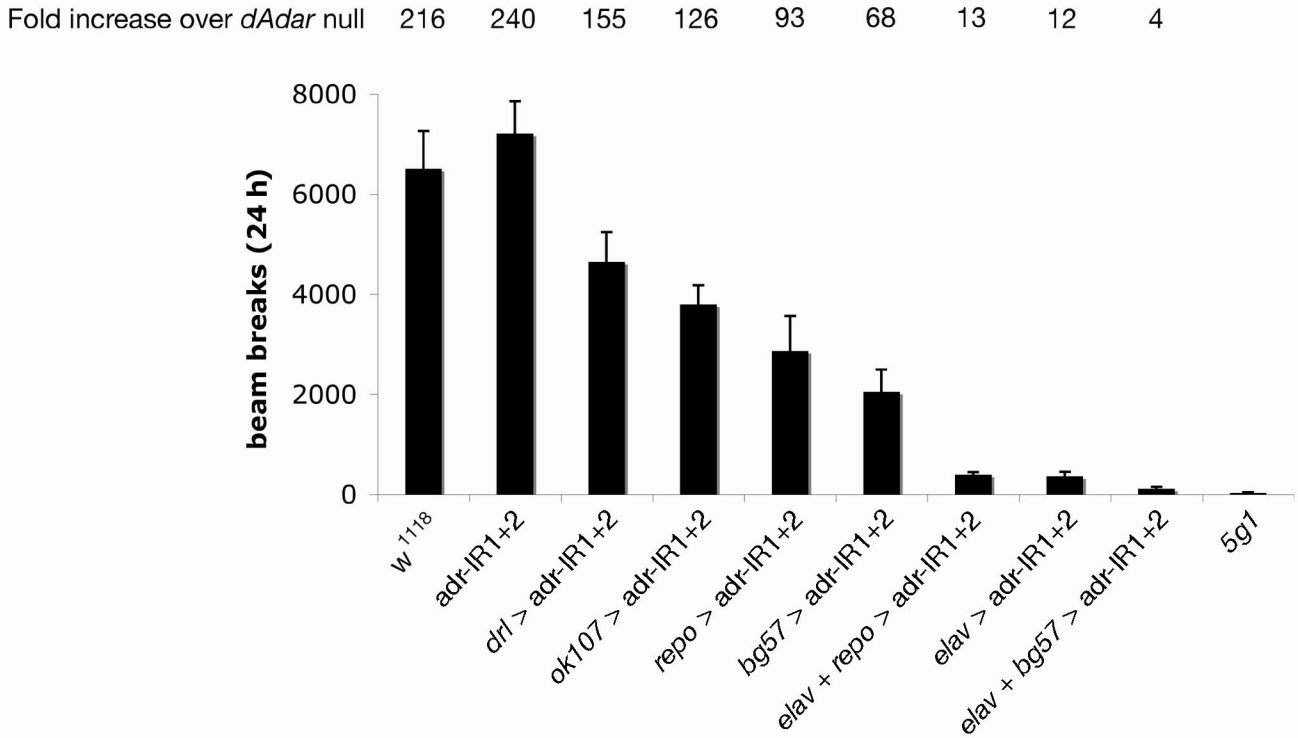

SUPPLEMENTARY FIGURE 3

A

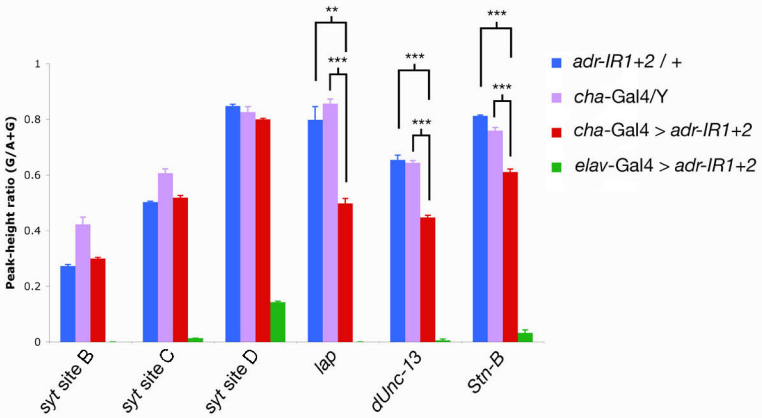

B

% Change in *cha*-Gal4 > *adr-IR1+2*

Relative to:	***syt* site B**	***syt* site C**	***syt* site D**	***lap***	***dUnc-13***	***Stn-B***
Transgenes/+	+ 9.9	+ 3.1	- 5.6	- 37.6	- 31.6	- 24.9
Driver/+	- 29.2	- 14.5	- 3.2	- 41.9	- 30.5	- 19.6

C

lap

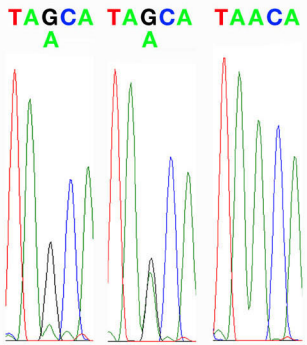

D

syt site D

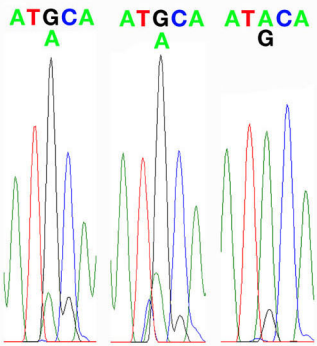

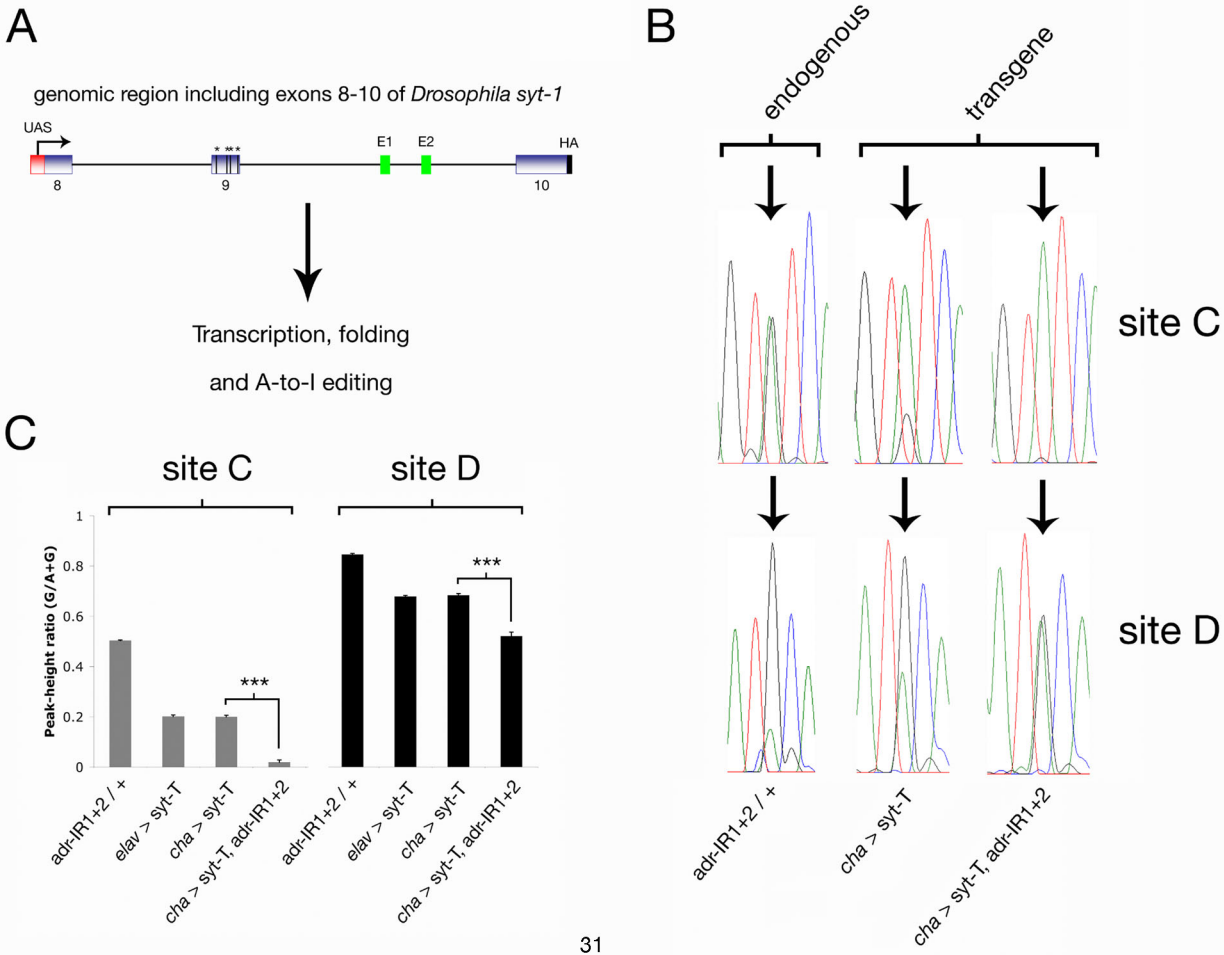
A
genomic region including exons 8-10 of Drosophila syt-1
UAS
E1
E2
HA
8
9
10
Transcription, folding
and A-to-I editing
B
endogenous
transgene
site C
site D
adr-IR1+2 / +
cha > syt-T
cha > syt-T, adr-IR1+2
C
site C
site D
Peak-height ratio (G/A+G)
1
0.8
0.6
0.4
0.2
0
***
***
adr-IR1+2 / +
elav > syt-T
cha > syt-T
cha > syt-T, adr-IR1+2
adr-IR1+2 / +
elav > syt-T
cha > syt-T
cha > syt-T, adr-IR1+2

SUPPLEMENTARY FIGURE 5

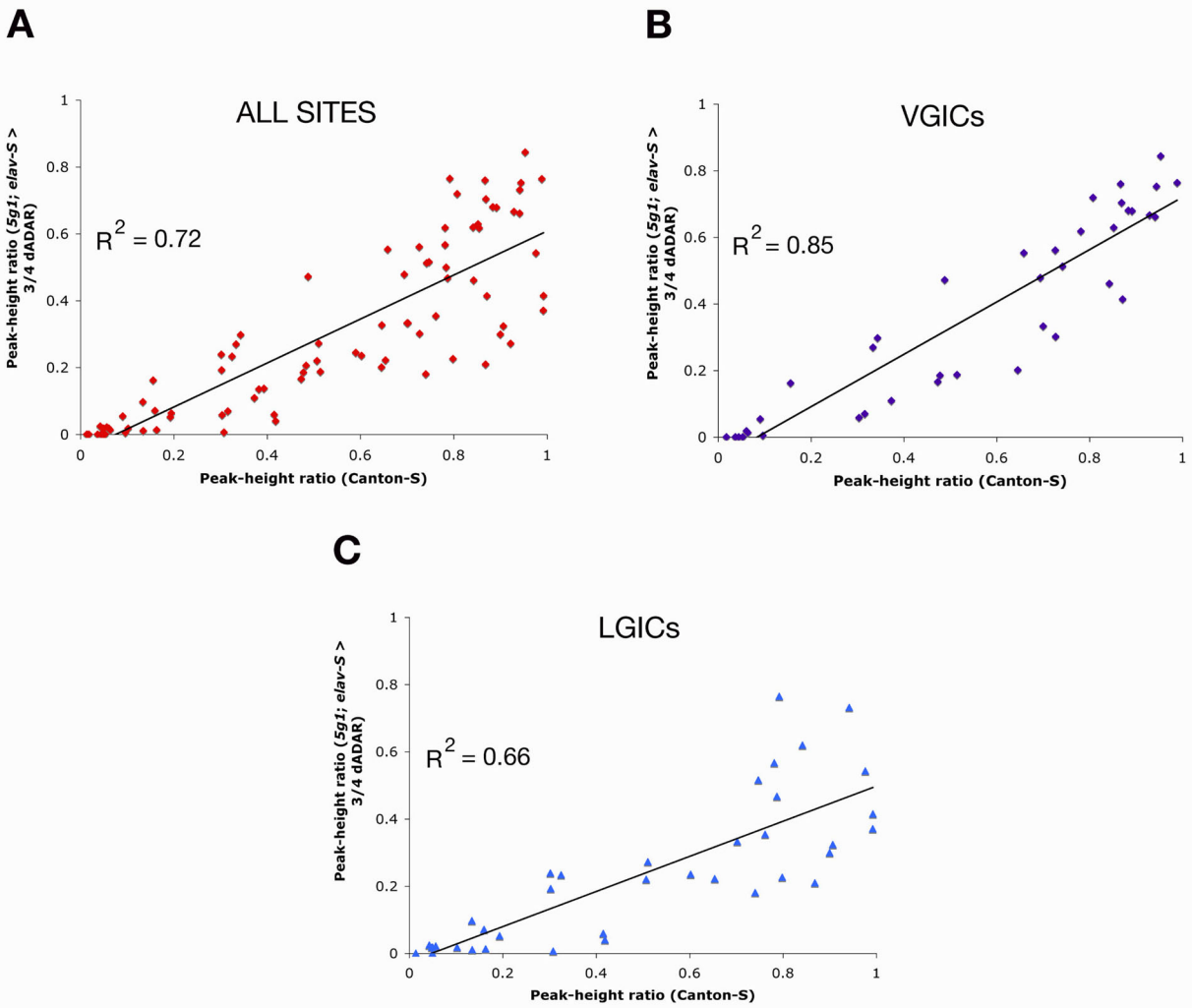

SUPPLMENTAY FIGURE 6